

## Microwave dielectric studies of the spin-density-wave state in $(\text{TMTSF})_2\text{PF}_6$

J. L. Musfeldt and M. Poirier

*Centre de Recherches en Physique du Solide, Département de Physique, Université de Sherbrooke, Sherbrooke, Québec, Canada J1K 2R1*

P. Batail and C. Lenoir

*Laboratoire de Physique des Solides, Université Paris-Sud, 91405 Orsay, France*

(Received 3 August 1994; revised manuscript received 20 October 1994)

We have investigated the 16.5 GHz microwave response of single-crystal samples of  $(\text{TMTSF})_2\text{PF}_6$  at temperatures from 1.7 to 15 K as a function of external magnetic field. For the magnetic field applied along the chain direction, the microwave response does not change with field. However, with the field along the hard ( $c^*$ ) axis direction, striking changes are observed below  $T_c$  in the microwave dielectric constant and conductivity. The 4 K feature, present with good amplitude in  $\sigma_1$  at zero field, moves toward higher temperature and dampens with increasing magnetic field; at  $H=10$  T, it has disappeared. The local maximum near 4 K in  $\sigma_1$  is accompanied by a sharp decrease in  $\epsilon_1$ . The orbital effects are discussed within the framework of quasiparticle effects on Fermi-surface nesting properties as well as within a model for magnetic-field effects on the spin-density-wave condensate. Emphasis is placed upon the analysis of the 4 K feature, the implications for the second spin-density-wave phase, and the possible relationship to a glassy transition.

### I. INTRODUCTION

The subject of broken symmetry ground states has received a great deal of attention in recent years. This interest has been exemplified by a large number of studies on charge-density-wave materials where the periodic modulation of charge is accompanied by a lattice distortion and the transition itself is driven by electron-phonon interactions.<sup>1-4</sup> More recent interest has concentrated on spin-density-wave (SDW) systems,<sup>5</sup> where the transition is brought about by electron-electron interactions and the rich variety of low-temperature phenomena are magnetic in origin. Despite this fundamental difference, numerous studies have noted a similar electromagnetic response in SDW and CDW phases.<sup>5-8</sup> Both systems are characterized by low-frequency internal deformations of the density wave, a low-energy collective mode (resonating at finite frequency due to impurity pinning), and an interband or interbandlike transition at higher energy.<sup>1,5</sup> Consequently, studies of SDW systems not only increase our understanding of the competition between magnetic and superconducting ground states, but they allow for a comparison of collective mode dynamics as well.

The Bechgaard family of organic salts [based upon tetramethyltetraselenafulvalene (TMTSF)] (Ref. 9) have been prototypical materials for the study of broken-symmetry SDW ground states. Of the Bechgaard salts, the  $\text{PF}_6$  compound has been the most extensively studied. Widely celebrated as an 0.9 K superconductor under modest pressure,<sup>10</sup>  $(\text{TMTSF})_2\text{PF}_6$  is metallic at ambient pressure, with a maximum dc conductivity of  $\approx 6 \times 10^4 \Omega^{-1} \text{cm}^{-1}$  just above 12 K.<sup>9</sup> The ultimate value of  $\sigma_1$  (as well as the transition temperature itself) is weakly dependent upon the counterion identity.<sup>9</sup> Structural studies show that the TMTSF molecules are slightly dimerized

along the chain axis ( $a$ ) of the material; transverse overlap integrals are weak but important enough to slightly warp the Fermi surface.<sup>11,12</sup>

The normal ( $T \geq 12$  K) state electromagnetic response of  $(\text{TMTSF})_2\text{PF}_6$  has been analyzed as a combination of a low-frequency Drude response and a temperature-independent gaplike feature in the far infrared.<sup>6,13,14</sup> The Drude relaxation time has been estimated to be of the order of  $3 \text{cm}^{-1}$ , putting  $(\text{TMTSF})_2\text{PF}_6$  in the clean limit at these temperatures.<sup>6</sup> The metallic nature of the  $\text{PF}_6$  salt is also revealed in the microwave dielectric properties as the low-frequency lossy response is not a function of frequency in the range 7–60 GHz.<sup>6,14-16</sup> The microwave results suggest that  $(\text{TMTSF})_2\text{PF}_6$  is in the dirty limit, in contrast to the optical estimate of  $\tau$  given above.

$(\text{TMTSF})_2\text{PF}_6$  undergoes an antiferromagnetic phase transition at  $\approx 12$  K, below which a series of instabilities develops. The strong anisotropy in the low-temperature magnetic susceptibility<sup>17,18</sup> combined with the absence of structural distortion at  $T_c$  (Refs. 19, 20) was crucial in distinguishing the broken-symmetry ground state in TMTSF compounds from that in CDW materials. The modulation of the spin density is weakly incommensurate with the lattice<sup>21</sup> and is given as  $S(r) = S_1 \cos(Q \cdot r + \phi)$ , where  $S_1$  and  $\phi$  are the SDW amplitude and phase, respectively. Impurity pinning causes the collective mode to resonate at finite frequencies. Upon application of an external electric field, the collective mode can be depinned and carry current.<sup>8,22,23</sup> TMTSF-based molecular crystals have been the subject of numerous experimental and theoretical studies,<sup>24-41</sup> due to the novel ground state.

NMR has been a powerful technique for probing the nature of the broken-symmetry ground state,<sup>21,42-49</sup> The spin-lattice relaxation time  $T_1^{-1}$ , displays a strong di-

vergence near 12 K due to critical SDW fluctuations,<sup>49</sup> whereas the relaxation in the ordered phase is presumably due to phason excitation.<sup>44–46</sup> The observation that the SDW phase can be divided into a series of subphases has generated a lot of interest.<sup>47,48</sup> From changes in the spin-lattice relaxation time, instabilities are observed at 12 K, 3.5 K, and 1.9 K at ambient pressure. This divides the phase diagram into three regimes, usually labeled SDW 1, SDW 2, and SDW 3, respectively. The sharp fall-off in  $T_1^{-1}$  near 3.5 K has recently been attributed to a slowing down of phason dynamics.<sup>44,45</sup> The application of a weak transverse magnetic field<sup>44</sup> does not seem to strongly affect the temperature at which the proton relaxation rate drops at low fields (0.35–0.9 T), but the transition temperature seems to move slightly higher for  $H = 1.48$  T. The disappearance of the Shubnikov–de Haas oscillations<sup>25</sup> in the same temperature range suggests a significant modification of the Fermi surface and perhaps a transition to a state without closed orbits. With increasing pressure, the SDW phase boundaries<sup>47</sup> display increasing downward curvature, with the low-temperature broken-symmetry states (SDW 2 and SDW 3) competing with the superconducting ground state.<sup>26,47</sup> Thus, interest has focused on factors which influence the competition between these two states, with the ultimate goal of stabilizing the superconducting state.

Specific heat studies of the 12 K transition in the  $\text{PF}_6$  salt<sup>50</sup> have shown that the thermodynamic response is not mean-field like and that the critical regime for three-dimensional (3D) fluctuations is on the order of 0.3 K. No change in the size of the fluctuation regime is detected in the presence of a transverse magnetic field, suggesting that the transverse coherence length of the SDW is unaffected by the field. Thermodynamic studies have also concentrated on the cascade of SDW transitions below  $T_c$ , correlating changes in the excess lattice specific heat with the three aforementioned SDW phases observed by NMR.<sup>51</sup> In particular, their results show that the transition near 3.5 K is weakly coupled to the lattice. More recently, thermal annealing calorimetric studies have suggested the intriguing possibility of a relaxational glass transition at low temperatures in the  $\text{PF}_6$  salt.<sup>52</sup>

The low-energy electromagnetic response of the TMTSF salts in the low-temperature phase can be characterized by three distinct contributions: internal deformations, the collective mode response, and the temperature-independent far-infrared feature.<sup>6,7,29,53</sup> The SDW phase of the  $\text{PF}_6$  salt has been the subject of numerous microwave investigations because of the proximity of the collective mode to this frequency regime. Early experiments conclusively measured excess conductivity in the SDW state at ac frequencies compared to dc and showed that the additional current-carrying capacity was due to the contribution of the collective mode.<sup>8,16,54</sup> The microwave resistivity displays an upturn at  $T_c$  and a continuous rise in the low-temperature phase, although the detailed features in the SDW state are unclear due to the difficulty of these first measurements. Later investigations showed that  $(\text{TMTSF})_2\text{PF}_6$  displays a strongly frequency-dependent response in the microwave and millimeter regimes; various structures ap-

pear in the microwave resistivity depending on the probe energy.<sup>6,14–16</sup> When the frequency response is measured at constant temperature, a clear Lorentzian signature of the collective mode is observed below  $T_c$ .<sup>13,53</sup> At 10 K, the resonance is centered at  $\approx 0.08$   $\text{cm}^{-1}$ ; the collective mode resonance moves out to higher energy ( $\approx 0.35$   $\text{cm}^{-1}$ ) at 2 K because impurity screening is reduced as the quasiparticle freeze out.<sup>13</sup> Presently, there are unresolved problems regarding the missing oscillator strength when the Drude contribution collapses to the collective mode at  $T_c$ .<sup>6,13,53,55</sup> More recent radio frequency dielectric studies<sup>52</sup> show that  $\epsilon_1$  displays a very slow low-temperature relaxation that is not well described by the typical activated behavior. Combined with the aforementioned specific heat effects, the shift in amplitude with decreasing frequency is attributed to a glass transition with a limiting value of 2 K. Despite these extensive studies, questions still exist regarding the microwave dielectric response of  $(\text{TMTSF})_2\text{PF}_6$  in the low-temperature phase. For instance, there is no information available on the thermal dependence of the dielectric constant at these frequencies. Furthermore, no microwave measurements have been done in the presence of an external magnetic field.

In order to provide further information on the nature of the 12 K phase transition and the underlying series of SDW instabilities, we have investigated the 16 GHz microwave response of  $(\text{TMTSF})_2\text{PF}_6$  as a function of temperature and applied magnetic field. Because the manner in which the dielectric properties change with temperature is a fundamental material property, such measurements provide an important low-frequency characterization of this series of phase transitions. We compare our zero-field results to previous reports on the microwave resistivity of  $(\text{TMTSF})_2\text{PF}_6$ , and suggest that the pronounced differences in the SDW state are related to the manner in which the data are treated. Furthermore, to our knowledge, this is the first report of magnetic-field effects on the SDW condensate in the  $\text{PF}_6$  salt as measured by a microwave probe. The strong magnetic-field effects observed in the dielectric response in the SDW regime below 12 K are likely to be essential to the complete understanding of the nature of the magnetic ground state in the TMTSF compounds and the driving forces of the SDW 1  $\rightarrow$  SDW 2 transition near 3.5 K.

## II. EXPERIMENTAL DETAILS

### A. Sample preparation

Single crystals of  $(\text{TMTSF})_2\text{PF}_6$  were grown by standard electrochemical methods. The shiny black needles had typical dimensions of  $\approx 0.25 \times 0.017 \times 0.0085$   $\text{cm}^3$ . For the measurement, a sample was positioned inside a quartz capillary and held in place with cotton threads to ensure that it did not turn out of the intended orientation. The encapsulated crystal was subsequently attached to a quartz rod which ran through the cavity, allowing the sample to be easily inserted into and with-

drawn from the cavity.

The samples were cooled slowly to 4 K to prevent microcracking and outright breakage, which was evidenced by a sharp increase in the resonance frequency. In general, crystals of the same batch yielded similar dielectric properties; however, we did notice changes in the SDW response (but not the normal state properties) after repeated cycling to room temperature. Consequently, thermal cycling was avoided and measurements were generally taken on an unannealed sample, if possible.

### B. Microwave cavity measurements

We used a microwave cavity perturbation technique to measure the complex dielectric function  $\epsilon^* = \epsilon_1 + i\epsilon_2$  of a  $(\text{TMTSF})_2\text{PF}_6$  single crystal as a function of temperature (in the range 1.7–15 K) and external magnetic field (0–10 T); here,  $\epsilon_1$  and  $\epsilon_2$  are the dielectric constant and the dielectric loss, respectively. The conductivity  $\sigma_1$  is related to the lossy response as  $\epsilon_0\epsilon_2\omega$ . For the measurements reported here, the microwave experiment was conducted in a rectangular copper cavity operated at 16.5 GHz in the  $\text{TE}_{102}$  transmission mode. Zero-field data were also collected at 13 GHz in the  $\text{TE}_{101}$  mode. All measurements were done with the electric-field vector parallel to the TMTSF chain axis direction. What we measure in this experiment is the perturbation of the resonance frequency ( $\frac{\delta\omega}{\omega}$ ) and the quality factor ( $\Delta\frac{1}{2Q}$ ) of the cavity upon insertion of the sample at the electric-field maximum ( $H_{\text{ac}} = 0$  here). These two parameters were measured at temperature intervals of 0.15 K between 1.7 and 15 K at a rate of 0.6 K/min in order to obtain the thermal dependence of the dielectric constant. A static external magnetic field could be applied along the chain axis ( $a$ ) or hard axis ( $c^*$ ) direction of the crystal. Using our apparatus, frequency and bandwidth changes can be measured with a sensitivity of better than 1 part in  $10^{-7}$ ; 5 mK precision was achieved in temperature control.

### C. Data analysis

The results were analyzed within the framework of the quasistatic approximation,<sup>56</sup> where the real and imaginary parts of the dielectric function are given as

$$\epsilon_1 = 1 - \frac{[\frac{\delta\omega}{\omega}(\frac{\delta\omega}{\omega} + \frac{\alpha}{N}) + (\Delta\frac{1}{2Q})^2]}{N[(\frac{\delta\omega}{\omega} + \frac{\alpha}{N})^2 + (\Delta\frac{1}{2Q})^2]} \quad (1)$$

and

$$\epsilon_2 = \left(\frac{\alpha}{N^2}\right) \frac{(\Delta\frac{1}{2Q})^2}{[(\frac{\delta\omega}{\omega} + \frac{\alpha}{N})^2 + (\Delta\frac{1}{2Q})^2]} \quad (2)$$

Here,  $N$  is the depolarization factor along the direction of the electric field and  $\alpha$  is the cavity filling factor. These parameters are determined from a knowledge of the sample and cavity geometry.<sup>57</sup> The quasistatic approxima-

tion is strictly valid when the field is uniform over the sample. In the case of our samples, the penetration depth is on the order of the sample thickness ( $\approx 8.5 \mu\text{m}$ ), suggesting that the quasistatic approximation is appropriate in this case.

This method contrasts the more common approach to the analysis of microwave cavity data,<sup>6,13–16,53,54,58,59</sup> where it is usual to relate the real part of the surface impedance to the “microwave resistivity” as

$$\rho = \frac{2R_s^2}{\mu_0\omega}. \quad (3)$$

Here,  $R_s$  is the surface resistance (which is determined solely from the lossy response),  $\mu_0$  is the permeability of free space, and  $\omega$  is the angular frequency. This expression derives from the more general relation

$$\Delta\frac{1}{2Q} + i\left(\frac{\alpha}{N} + \frac{\delta\omega}{\omega}\right) = \beta(R_s + iX_s), \quad (4)$$

where  $X_s$  is the surface reactance and  $\beta$  is a constant related to sample and cavity geometry. If  $\sigma_1 \gg \sigma_2$ ,  $R_s = X_s = (\mu_0\omega/2\sigma_1)^{1/2}$ . The surface impedance framework is very useful when considering highly conducting samples of sufficient thickness, but one must demonstrate that  $X_s = R_s$  in order to employ it. Neglect of the surface reactance term  $X_s$  is generally a practical consideration, resulting from the difficulty of an accurate measurement of  $\frac{\delta\omega}{\omega}$ .<sup>6,53,58</sup> We are not limited by constraints on the precision of  $\frac{\delta\omega}{\omega}$  here. Our measurements (on these samples) show that  $R_s$  and  $X_s$  cannot be placed in perfect coincidence, even in a limited temperature range near 12 K (Fig. 1). The different temperature dependence of  $R_s$  and  $X_s$  (both above and below  $T_c$ ) demonstrates the importance of the frequency response in the description of  $\epsilon_1$  and  $\sigma_1$  and the broad inapplicability of the “microwave resistivity” approximation to our samples.

A previous and independent determination of the temperature-dependent thermal expansion in the  $a$  crystallographic direction<sup>19,20</sup> allows us to account for

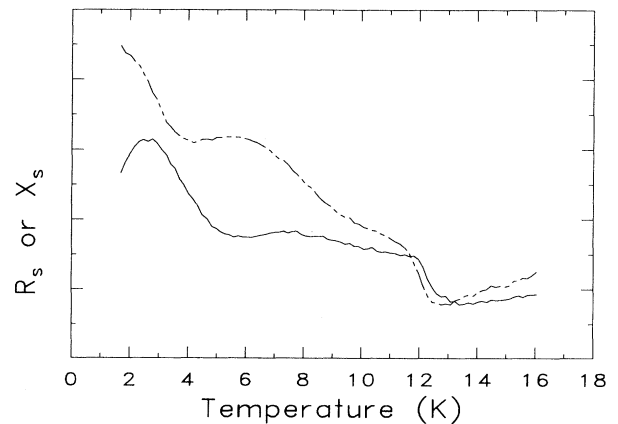


FIG. 1. The surface resistance (solid line) and the surface reactance (double-dashed line) of  $(\text{TMTSF})_2\text{PF}_6$  as a function of temperature at 16.5 GHz. The lack of long-range coincidence of  $R_s$  and  $X_s$  indicates the inapplicability of the surface impedance approximation in our samples.

changes in sample geometry with temperature.<sup>60</sup> We correct the experimental frequency shift using a Taylor series expansion of the sample length as  $(\frac{\delta\omega}{\omega})_{\text{new}} = (\frac{\delta\omega}{\omega})_{\text{expt}}(1 - 3\frac{\Delta\alpha}{\alpha})$ . It should be noted that  $\frac{\Delta\alpha}{\alpha}$  varies smoothly with temperature,<sup>19,20</sup> and so no additional “features” were introduced as a result of this procedure.

A proper accounting of the frequency shift within the quasistatic approximation relies not only on an accurate measurement of  $\frac{\delta\omega}{\omega}$ , but also upon a realistic choice of  $\frac{\alpha}{N}$ . This is because it is the *difference* between these two quantities ( $\frac{\delta\omega}{\omega}$  is negative) that appears in Eqs. (1) and (2). Our method for determining  $\frac{\alpha}{N}$  is as follows. First, we calculate  $\frac{\alpha}{N}$  from a knowledge of sample dimensions by approximating the sample geometry as a prolate ellipsoid.<sup>57</sup> Second, we choose the level of  $\frac{\alpha}{N}$  with respect to the expansion-corrected frequency shift. The fact that  $\frac{\alpha}{N}$  is the limiting value of  $\frac{\delta\omega}{\omega}$  in the case of infinite conductivity allows us to attach a lower bound to the relative level of this curve. The expansion-corrected frequency shift itself provides also a hint for the level of  $-\frac{\alpha}{N}$ , as it displays a clear change of slope at  $T_c$ . We illustrate this behavior in the upper panel of Fig. 2. The level of  $\frac{\alpha}{N}$  which reproduced the thermal dependence of the normal state dc conductivity was determined to be the optimal choice.

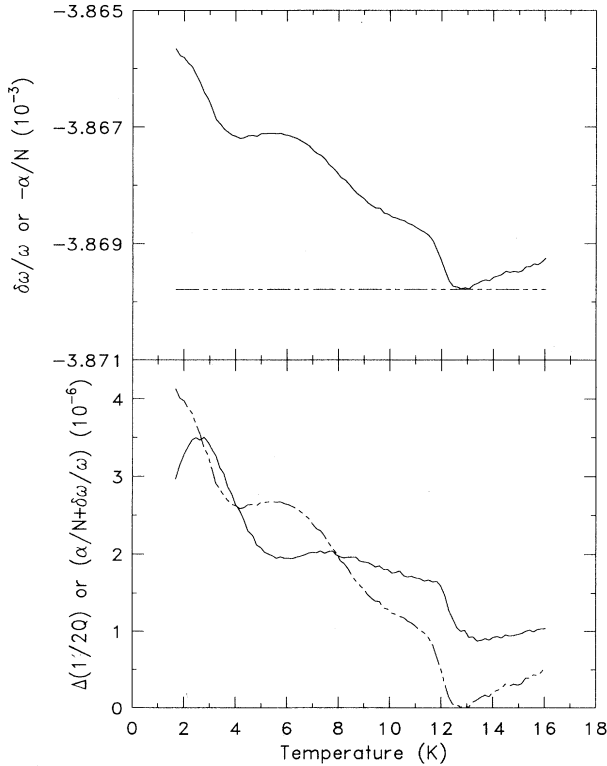


FIG. 2. Upper panel:  $\frac{\delta\omega}{\omega}$  of  $(\text{TMTSF})_2\text{PF}_6$  corrected for thermal expansion (solid line) as a function of temperature at 16.5 GHz. The double-dashed line shows our selection of  $-\frac{\alpha}{N}$ . Lower panel:  $\Delta(\frac{1}{2Q})$  (solid line) and  $(\frac{\alpha}{N} + \frac{\delta\omega}{\omega})$  (double-dashed line) as a function of temperature at 16.5 GHz.

The expansion-corrected frequency shift seems to diverge from  $-\frac{\alpha}{N}$  above  $T_c$ , suggesting that  $\epsilon_1$  may be accessible in the normal state even though the conductivity is high. However, the error bars on this quantity are large because  $\Delta(\frac{1}{2Q})$  and  $(\frac{\alpha}{N} + \frac{\delta\omega}{\omega})$  are small and of similar magnitude. In addition, any measurement uncertainty in the frequency shift or thermal expansion will be magnified because we are taking the difference between two small quantities to calculate  $(\frac{\alpha}{N} + \frac{\delta\omega}{\omega})$ . The size of the error bars on  $\epsilon_1$  in the high-temperature phase also depends on how  $\frac{\alpha}{N}$  is chosen. Small changes in  $\frac{\alpha}{N}$  do not modify the overall temperature dependence of the dielectric response below  $T_c$ .

With this choice of  $\frac{\alpha}{N}$ , the term  $(\frac{\alpha}{N} + \frac{\delta\omega}{\omega})$  is finite in the normal state and climbs steeply in the SDW phase. It is small near the transition, nearly equal in magnitude to the  $\Delta(\frac{1}{2Q})$  term at intermediate temperatures (7–10 K), and it grows to dominate the response of  $\epsilon_1$  and  $\sigma_1$  at low temperatures (below 4 K). Some typical zero-field data are displayed in the lower panel of Fig. 2.

### III. RESULTS

#### A. Zero-field measurements

In this section, we present the zero-field temperature profile of the microwave dielectric properties of  $(\text{TMTSF})_2\text{PF}_6$  as calculated using the quasistatic approximation. Our discussion concentrates on a comparison with previous data.

The expansion-corrected frequency shift, shown in the upper panel of Fig. 2, is characterized by a small positive slope in the normal state, a sharp change of slope at  $T_c$ , and a steady ascent in the SDW state, with a change in curvature near 8 K and a pronounced depression centered near 4 K. The local minimum near 4 K is present with good amplitude in all of our samples; it is about 2 K wide at zero field. The change in bandwidth at 16.5 GHz is shown in the lower panel of Fig. 2. It is characterized by a sharp increase at  $T_c$ , a plateau region between 5 and 11 K (punctuated by a local maximum near 8 K), and a strongly increasing absorption below 5 K;  $\Delta(\frac{1}{2Q})$  decreases again below 2.5 K. Certain variations in the raw data arise from sample to sample due to differences in crystal geometry. When the data are mixed together to yield  $\sigma_1$  and  $\epsilon_1$ , similar properties are obtained.

Figure 3 displays the thermal dependence of the 16.5 GHz conductivity. In the normal state, the microwave conductivity is high and within an order of magnitude of the value obtained from previously reported dc measurements.<sup>9,22</sup> After a sharp drop at 12 K,  $\sigma_1$  decreases gradually. In agreement with previous ac experiments,<sup>5</sup> the microwave conductivity is more than an order of magnitude higher than the dc conductivity due to the current-carrying capacity of the collective mode. Thus, the quasi-particle contribution to the conductivity is small in the low-temperature phase and the microwave conductivity is dominated by the collective mode response. A local maximum is observed near 4 K,

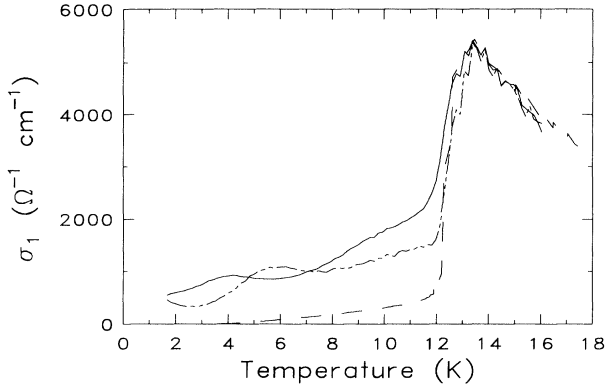


FIG. 3. 16.5 GHz conductivity of  $(\text{TMTSF})_2\text{PF}_6$  calculated within the quasistatic approximation (solid line) and inverse of the “microwave resistivity” (double-dashed line) as a function of temperature. The dc conductivity (dashed line) is also shown. Note that the level of  $1/\rho_{\text{micro}}$  and  $\sigma_{\text{dc}}$  has been normalized to our data at 12 K.

which is absent when  $\frac{\delta\omega}{\omega}$  is neglected from the analysis. Zero-field measurements at 13 GHz confirm the presence of this structure. We will discuss the 4 K feature at length in subsequent sections.  $\sigma_1$  begins to decrease near 3.5 K. Because the dc (single-particle) conductivity is featureless in the SDW regime, the 3.5 K structure must be related to condensate effects. Ideally, upon subtraction of the quasiparticle contribution, we could isolate the SDW contribution to the conductivity. Unfortunately, dc conductivity measurements are not available for our samples.

Considering the large number of dielectric studies that have been undertaken on TMTSF systems during the past decade, it is worthwhile to compare our conductivity data with earlier results. To illustrate the difference, we have calculated the “microwave resistivity” in the manner of previous authors and plotted it ( $\sigma_{\text{micro}} = 1/\rho_{\text{micro}}$ ) along side our data and the scaled dc conductivity of Tomić *et al.*<sup>22</sup> in Fig. 3.

The inverse of the “microwave resistivity,” calculated with the simplified analysis of Eq. (3),<sup>6,13–16,53,54,58,59</sup> is in reasonable agreement with previously reported results. However, the overall shape of  $1/\rho_{\text{micro}}$  is unlike that which is obtained from an analysis based upon the full quasistatic approximation particularly at low temperature. The curves in Fig. 3 highlight the fact that  $\sigma_1$  contains more than just  $\Delta(\frac{1}{2Q})$ ; it is a complicated function which must include both the frequency *and* the bandwidth contributions to account for the total dissipation. Furthermore, by analyzing only the lossy response, the aforementioned authors are unable to determine the real part of the dielectric constant  $\epsilon_1$ .

We display the zero-field 16.5 GHz dielectric constant of  $(\text{TMTSF})_2\text{PF}_6$  (together with data taken in the presence of a transverse magnetic field) in Fig. 4. At 16.5 GHz,  $\epsilon_1$  is large ( $\approx 10^5$ ), consistent with the highly polarizable nature of the condensate at this frequency and in reasonable agreement with the trend expected from radio frequency dielectric measurements<sup>7,52</sup> as well as

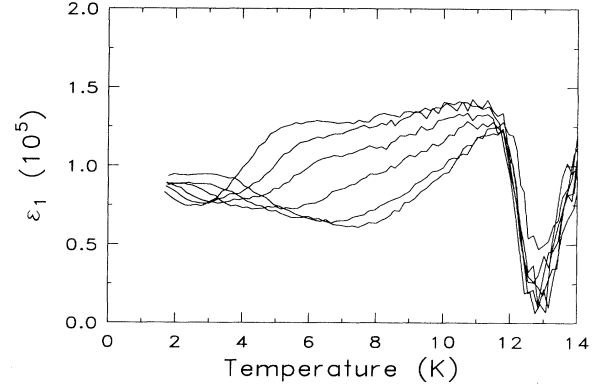


FIG. 4. 16.5 GHz dielectric constant of  $(\text{TMTSF})_2\text{PF}_6$  as a function of temperature and applied magnetic field. The external magnetic field ( $H = 0, 1, 2, 4, 7, 10$  T) is applied along the hard axis ( $c^*$ ) direction. Curves change monotonically with increasing  $H$ .

previous microwave studies.<sup>16,61</sup> In the low-temperature phase, the zero-field curve displays a plateau at intermediate temperatures, a sharp drop near 4 K (concomitant with the local maximum in the lossy response), and a slight upturn at lower temperatures. We attribute the sharp increase of  $\epsilon_1$  at  $T_c$  to the opening of the SDW gap. Similar behavior was observed at 13 GHz. Because  $R_s \neq X_s$  (Fig. 1), it appears that  $\epsilon_1$  may be accessible in the normal state as well. However, we have no explanation for the unexpected rise of  $\epsilon_1$  above 12 K. As discussed in Sec. II C, significant errors in this quantity are likely to be present in the normal state. Thus, we do not consider the thermal dependence of  $\epsilon_1$  reliable in this regime.

## B. Magnetic-field effects

In this section, we present the change in frequency and bandwidth, as well as the dielectric response, as a function of temperature and magnetic field for  $(\text{TMTSF})_2\text{PF}_6$  at 16.5 GHz. Here, we consider two separate cases:  $H \parallel c^*$  and  $H \parallel a$ . Our later discussion concentrates primarily on the data taken in the presence of the transverse field ( $\perp$  to the conducting planes), as it is the most interesting.

### 1. $H$ along the hard axis direction

The experimental frequency shift and the change in bandwidth as a function of external magnetic field along the hard axis direction ( $c^*$ ) of the TMTSF crystal are displayed in the upper and lower panels of Fig. 5, respectively. The clear correlations once again emphasize the fact that  $\frac{\delta\omega}{\omega}$  and  $\Delta(\frac{1}{2Q})$  are not independent quantities.

Referring to the upper panel of Fig. 5, the magnetic-field dependence of  $\frac{\delta\omega}{\omega}$  is quite strong at low tempera-

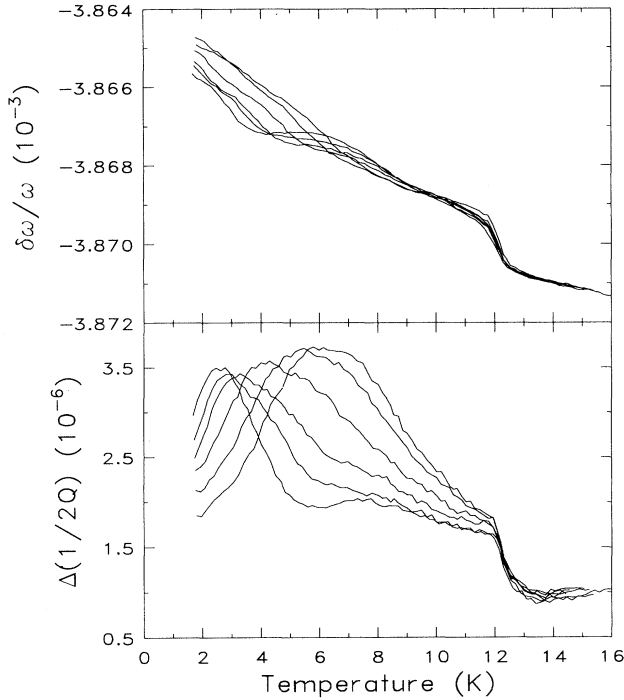


FIG. 5. Upper panel: experimental  $\frac{\delta\omega}{\omega}$  as a function of temperature and magnetic field at 16.5 GHz. Lower panel:  $\Delta(\frac{1}{2Q})$  as a function of temperature and magnetic field at 16.5 GHz. The external magnetic field ( $H = 0, 1, 2, 4, 7, 10$  T) is applied along the hard axis ( $c^*$ ) direction. Curves change monotonically with increasing  $H$ .

ture. With increasing field, the pronounced depression centered near 4 K broadens and shifts to higher temperature; at the same time, the amplitude weakens considerably. The largest changes in the behavior of the 4 K feature occur at lower fields ( $H \leq 4$  T). At  $H = 10$  T, we detect no trace of the depression in the frequency response.

Referring to the lower panel of Fig. 5, the striking changes in the dissipation as a function of applied magnetic field can be characterized as the movement of absorption amplitude to higher temperature. This process is illustrated by the behavior of the 2 K maximum in the  $H = 0$  curve of  $\Delta(\frac{1}{2Q})$ , which broadens, shifts slightly downward in position, and subsequently moves to higher temperature with increasing field. At the same time, the zero-field minimum near 5.5 K becomes less pronounced and moves, in concert with the 2 K maximum, to higher temperature with increasing field. By  $H = 4$  T, the small local maximum near 8 K is lost. At 10 T,  $\Delta(\frac{1}{2Q})$  displays only a broad maximum near 5.5 K. In the normal state,  $\Delta(\frac{1}{2Q})$  rises with increasing field, indicative of the magnetoresistance in the microwave conductivity (Fig. 6).

The 16.5 GHz conductivity and dielectric constant as a function of temperature and magnetic field are shown in Figs. 4 and 6. For the conductivity (Fig. 6), we display only the  $H = 0$  and 10 T curves to better highlight the observed differences in  $\sigma_1$ , particularly with regard

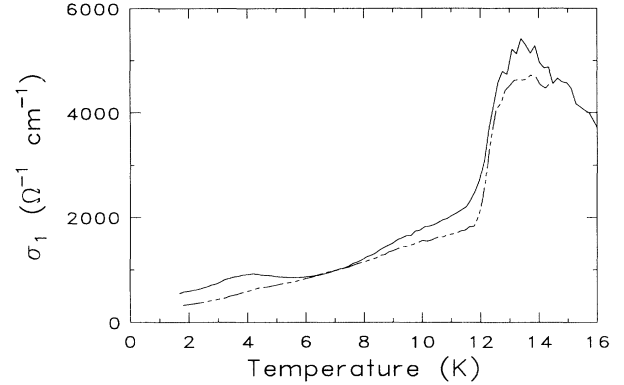


FIG. 6. 16.5 GHz conductivity of  $(\text{TMTSF})_2\text{PF}_6$  as a function of temperature and applied magnetic field. Solid line,  $H = 0$ ; double-dashed line,  $H = 10$  T. The external magnetic field is applied in the hard axis ( $c^*$ ) direction.

to the interesting low-temperature feature. In Fig. 4, we show several curves taken at different fields to display the progressive changes in  $\epsilon_1$  with  $H \parallel c^*$ . In the following paragraphs, our comments will refer first to the conductivity and then to the dielectric constant.

The application of the magnetic field in the hard axis direction has a pronounced effect on the normal state microwave properties of  $\sigma_1$ . At 14 K, we observe a normal state microwave magnetoresistance of about 14% at 10 T, somewhat less than previous dc measurements.<sup>30</sup> The magnetic-field dependence of the transition temperature is also of interest, as it provides insight into the nature of the nesting transition and the role of the spins. Within a variety of theoretical frameworks,<sup>37–39</sup>  $T_c$  is predicted to increase as  $H^2$ ; such an increase is usually taken as an indication of an improvement in Fermi-surface nesting. Our experimental accuracy is not high enough to distinguish such a functional form from any other, as our data were taken at temperature intervals of 0.15 K. However, it is clear that  $T_c$  does increase slightly with  $H$  applied along the hard axis direction; we find that  $\delta T$  is typically  $\approx 0.2$  K at 10 T.

In the low-temperature phase, the microwave response is dominated by the collective mode; the quasiparticle contribution to  $\sigma_1$  is small, as evidenced by the low dc conductivity. Directly below the 12 K transition, the magnitude of the 16.5 GHz magnetoresistance is significantly less than that reported in dc measurements.<sup>23,30</sup> We find that  $\sigma_1$  differs from the zero-field level by a factor of  $\approx 1.3$ , compared with a factor of 20 in the dc experiment. In zero field, the 3–4.5 K regime is characterized by a small local increase in the conductivity, signaling the approach to the SDW 1  $\rightarrow$  SDW 2 transition. Because the quasiparticle conductivity is featureless at low temperature,<sup>23,30</sup> this behavior must be related to the collective mode response. With increasing magnetic field, the structure broadens, weakens, and moves to higher temperature, likely defining a phase boundary between SDW 1 and SDW 2.<sup>47</sup> As shown in Fig. 6, the local maximum has completely disappeared at 10 T. Near

7 K, the two curves in Fig. 6 are slightly inverted. The small crossover is likely due to amplitude originally associated with the 4 K depression in  $\frac{\delta\omega}{\omega}$  which has moved out toward 7 K with applied field (upper panel, Fig. 5). Below the SDW 2 transition (3.5 K), the microwave conductivity is characterized by a gradual but continuous decrease;  $\sigma_1$  is lower overall in the presence of the 10 T transverse magnetic-field.

The magnetic-field dependence of  $\epsilon_1$  is shown in Fig. 4. In the SDW state, the zero-field curve of the dielectric constant appears relatively flat at intermediate temperatures (5–10 K) with a strong decrease near 4 K and a narrow minimum centered at 2.5 K. With increasing field, the sharp drop in  $\epsilon_1$  weakens and moves to higher temperature, tracking the 4 K feature in  $\sigma_1$ . The width of the anomaly increases considerably as well, indicating a reduced sample polarizability in the presence of the field. There appears to be little systematic field dependence to  $\epsilon_1$  in the normal state, as might be expected considering the size of the error bars here.

## 2. $H$ along the chain axis

The experimental frequency shift and the change in bandwidth as a function of external magnetic field along the TMTSF chain direction ( $a$ ) are displayed in the upper and lower panels of Fig. 7, respectively. No significant

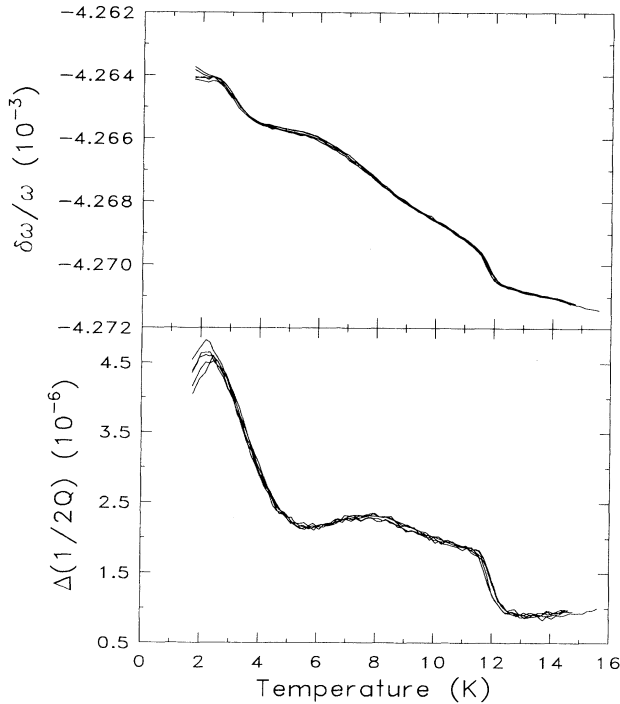


FIG. 7. Upper panel: experimental  $\frac{\delta\omega}{\omega}$  as a function of temperature and magnetic field at 16.5 GHz. Lower panel:  $\Delta(\frac{1}{2Q})$  as a function of temperature and magnetic field at 16.5 GHz. The external magnetic field ( $H = 0, 1, 2, 4, 7, 10$  T) is applied along the TMTSF chain axis ( $a$ ) direction.

magnetic-field dependence of these experimental quantities was observed. (We believe that the small changes below 2 K are due to minor sample misalignment with respect to  $H$ .)

Due to the absence of field effects on  $\frac{\delta\omega}{\omega}$  and  $\Delta(\frac{1}{2Q})$  in the  $H \parallel a$  configuration, no magnetic-field dependence is obtained in either  $\sigma_1$  or  $\epsilon_1$ . Both quantities display the same behavior as the zero-field curves shown in Figs. 4 and 6. Despite the lack of field dependence in the dielectric response, two interesting observations can be made. First, with the external magnetic field along the TMTSF chain direction, no microwave magnetoresistance was detected in the normal state or SDW state at 16.5 GHz, in agreement with previous dc results<sup>30</sup> (although a more limited temperature range was explored in those measurements). Second, within our experimental error,  $T_c$  does not change with magnetic field in agreement with recent calculations,<sup>62</sup> but in contrast to data obtained in earlier magnetic susceptibility measurements which reported a slight increase in  $T_c$  for  $H \parallel a$ .<sup>17</sup> We have no explanation for this discrepancy.

It is well known that the effect of an applied magnetic field is to confine the electrons in the direction orthogonal to the field, thus reducing the overall dimensionality of the system. The fact that no changes were observed in the two experimental quantities  $\frac{\delta\omega}{\omega}$  and  $\Delta(\frac{1}{2Q})$  as a function of  $H$  indicates that the external field produces no additional localization when applied along the TMTSF chain axis direction. This is because motion along  $c^*$  is incoherent due to the small value of the hopping integral ( $t_{c^*} \ll 10$  K).<sup>12</sup> Thus, further confinement results in limited change to the dielectric response.

## IV. DISCUSSION

First, we consider the Fermi-surface nesting problem and the direct role of free carriers in determining the dielectric response in  $(\text{TMTSF})_2\text{PF}_6$ .<sup>39–41</sup> Within this model, a gap forms in part of the Fermi surface below  $T_c$ , although pockets of electrons and holes may remain gapless due to imperfect nesting conditions.<sup>38–41,63</sup> The sharp drop of the microwave conductivity at  $T_c$  and the gradual decrease of  $\sigma_1$  in the SDW phase are in qualitative agreement with what one might expect from the opening of a spin-wave gap at 12 K and the gradual freezing out of remaining free carriers at lower temperature. The sharp increase in  $\epsilon_1$  through  $T_c$  clearly demonstrates that quasiparticle effects dominate the dielectric response in the normal state. However, our results are in contrast to what is typically observed at a metal-insulator transition in a CDW system (such as the perylenes),<sup>64</sup> where  $\epsilon_1$  rises rapidly at  $T_c$  and then drops rapidly as the gap opens fully in the low-temperature phase. This difference implies that the low-temperature dielectric response in the  $\text{PF}_6$  salt is due to more than free carrier effects. Application of a transverse magnetic field<sup>33,38–40,65,66</sup> acts to reduce the interchain overlap integrals and improve Fermi-surface nesting. With  $H \parallel c^*$ , the 16.5 GHz conductivity (Fig. 6) is reduced in the temperature regime

just below  $T_c$ . Whether the magnetoresistance in the condensed phase just below  $T_c$  is a residual effect (left over from the normal state) or distinct in its own right is still an open question, but in either case, it is orbital in nature. The increased transition temperature with applied field ( $H \parallel c^*$ ) is also consistent with this proposal.

There has been some discussion in the past that the 3.5 K phase transition (SDW 1  $\rightarrow$  SDW 2) might be a second nesting transition, perhaps to a ground state with a slightly different wave vector,<sup>40,47</sup> accompanied by a change in orbital motion.<sup>25</sup> However, if the local maximum in  $\sigma_1$  (or the corresponding sharp drop in  $\epsilon_1$ ) is taken to represent a boundary between the two condensed phases, the strong stabilization of SDW 2 (at the expense of SDW 1) in the magnetic field is quite rapid, suggesting that the 3.5 K feature is not a nesting transition in the same spirit as the metal  $\rightarrow$  insulator transition at  $T_c$ . That the anomaly moves to higher temperature with increasing field is in agreement with the trend expected from NMR measurements,<sup>44,47</sup> but in apparent contrast to the disappearance of the high field Shubnikov-de Haas oscillations<sup>25</sup> at 3.8 K. Recent theoretical work, based upon a changing wave vector from SDW 1  $\rightarrow$  SDW 2, has also proven unsatisfying.<sup>38</sup>

The large value of  $\epsilon_1$  in the low-temperature phase and the strong dispersion near 4 K suggests that the dielectric response of the (TMTSF)<sub>2</sub>PF<sub>6</sub> salt is due to more than just quasiparticle effects. The absence of structure in the dc conductivity<sup>23</sup> also shows that the role of quasiparticles is minimal here. Thus, a recent report by Bjeliš and Maki<sup>35</sup> is interesting, as it shows that local impurities and thermal fluctuations alone can deform the SDW and change the spatial and phase variations of the gap. Such local variations are stabilized in the presence of a magnetic field. The fluctuations lead (independently of Fermi nesting considerations) to orbital coupling effects, which increase linearly with applied field. Thus, within this model,  $H$  acts directly on the *condensate* to induce *a-b* plane orbital effects.

Because the condensate fraction increases with decreasing temperature, we expect to most easily distinguish condensate from quasiparticle effects at low temperature.<sup>37</sup> To this end, the drop in  $\epsilon_1$  near 4 K is an excellent candidate for consideration within the model of Bjeliš and Maki. However, the weakening (rather than strengthening) of the 4 K structure with  $H$  is an unexpected complication, and suggests that magnetic-field effects on the condensate polarizability are not completely understood.

A final possibility for the physical origin of the changing condensate behavior near 3.5 K in (TMTSF)<sub>2</sub>PF<sub>6</sub> has been suggested by Lasjaunias *et al.*<sup>52</sup> The authors recently presented a low-frequency dielectric study in which the behavior of (TMTSF)<sub>2</sub>PF<sub>6</sub> near 3.5 K is shown to be characteristic of a relaxational transition in a glassy material. The relaxation time displays a critical slowing down at low frequencies (less than 500 kHz) to a limiting value of  $\approx 2$  K.<sup>61</sup> Within the proposed model of the glassy phase, the SDW is pinned on random impurities, but there are clusters where the phase is coherent.<sup>52</sup> It is the large domain structure which is responsible for the

low-frequency relaxation, with the mean relaxation time dependent upon the average size of the cluster.

The aforementioned maximum in  $\epsilon_1$  is absent in our microwave dielectric data, suggesting that there may be one part of  $\epsilon_1$  which saturates at low frequency (perhaps related to the slow cooperative relaxation of large SDW domains and internal deformations) and another part which we are measuring at 16.5 GHz. The lower-energy cooperative motion is not observed because the long-range relaxation cannot follow the comparatively high-frequency perturbation used in our measurements.<sup>67-71</sup> Thus, the higher-frequency measurement would be expected to provide the more local probe of the collective mode polarization. Magnetic-field effects provide an additional complicating factor to the interpretation of low-frequency dielectric data. The application of an external magnetic field will affect the phase coherence inside the cluster, likely changing the characteristic length over which the SDW is pinned.

## V. CONCLUSION

We have reported the 16.5 GHz dielectric response of the quasi-one-dimensional Bechgaard salt (TMTSF)<sub>2</sub>PF<sub>6</sub> at temperatures above and below the 12 K antiferromagnetic phase transition as a function of external magnetic field. Data were collected with the magnetic field along the TMTSF chain direction as well as along the hard axis direction.

For the magnetic field applied along the chain direction, the microwave response of (TMTSF)<sub>2</sub>PF<sub>6</sub> does not change with field. That the magnetic field fails to induce additional localization effects is due to the strong anisotropy in the band structure. However, with the field along the hard axis direction, striking changes are observed in the microwave dielectric constant and conductivity. Our discussion has concentrated on the relationship between the dielectric features and the interesting series of instabilities which develop at low temperature. While quasiparticle effects are important in the normal state and at the 12 K transition, condensate effects dominate the dielectric response below  $T_c$ . Although it remains to understand the observed magnetic-field dependence of the 4 K feature, the transition seems to define a phase boundary between SDW 1 and SDW 2.

A more general question arises as to the relationship between the 4 K maximum and the 3.5 K falloff in the 16.5 GHz microwave conductivity and that observed via other experimental techniques, particularly the low-frequency dielectric response.<sup>25,44,45,47,51,52</sup> It would be fortuitous if the various signatures near the SDW 1  $\rightarrow$  SDW 2 transition were independent. Thus, the unification of these observations is a powerful motivation for further study of the TMTSF-based charge transfer salts.



## ACKNOWLEDGMENTS

This work was supported by grants from the Natural Science and Engineering Research Council of Canada (NSERC) and the Fonds pour la Formation de

Chercheurs et l'Aide à la Recherche (FCAR) of the Government of Québec. We greatly appreciate the technical assistance of M. Castonguay, as well as helpful conversations with C. Bourbonnais and G. Grüner and useful correspondence with A. Bjeliš and F. Nad.

- <sup>1</sup> G. Grüner, *Rev. Mod. Phys.* **60**, 1129 (1988).
- <sup>2</sup> A.J. Heeger, S. Kivelson, J.R. Schrieffer, and W.-P. Su, *Rev. Mod. Phys.* **60**, 782 (1988).
- <sup>3</sup> R.J. Donohoe, L.A. Worl, C.A. Arrington, A. Bulou, and B.I. Swanson, *Phys. Rev. B* **45**, 13 185 (1992).
- <sup>4</sup> F.H. Long, S.P. Love, B.I. Swanson, and R.H. McKenzie, *Phys. Rev. Lett.* **71**, 762 (1993).
- <sup>5</sup> G. Grüner, *Rev. Mod. Phys.* **66**, 1 (1994).
- <sup>6</sup> S. Donovan, Y. Kim, L. Degiorgi, M. Dressel, and G. Grüner, *Phys. Rev. B* **49**, 3363 (1994).
- <sup>7</sup> G. Mihály, Y. Kim, and G. Grüner, *Phys. Rev. Lett.* **67**, 2806 (1991).
- <sup>8</sup> P.A. Lee, T.M. Rice, and P.W. Anderson, *Solid State Commun.* **14**, 703 (1974).
- <sup>9</sup> K. Bechgaard, C.S. Jacobsen, K. Mortensen, H.J. Pederson, and N. Thorup, *Solid State Commun.* **33**, 1119 (1980).
- <sup>10</sup> D. Jérôme, A. Mazaud, M. Ribault, and K. Bechgaard, *J. Phys. (Paris) Lett.* **41**, L-95 (1980).
- <sup>11</sup> N. Thorup, G. Rindorf, H. Soling, and K. Bechgaard, *Acta Crystallogr. B* **37**, 1236 (1981).
- <sup>12</sup> T. Ishiguro and K. Yamaji, in *Organic Superconductors*, edited by P. Fulde, Springer Series of Solid State Sciences Vol. 88 (Springer-Verlag, Berlin, 1990).
- <sup>13</sup> S. Donovan, Y. Kim, L. Degiorgi, and G. Grüner, *J. Phys. (France) I* **3**, 1493 (1993).
- <sup>14</sup> S. Donovan, L. Degiorgi, and G. Grüner, *Europhys. Lett.* **19**, 433 (1992).
- <sup>15</sup> H.H.S. Javadi, S. Sridhar, G. Grüner, L. Chiang, and F. Wudl, *Phys. Rev. Lett.* **55**, 1216 (1985).
- <sup>16</sup> A. Zettl, G. Grüner, and E.M. Engler, *Phys. Rev. B* **25**, 1443 (1982).
- <sup>17</sup> K. Mortensen, Y. Tomkiewicz, T.D. Schultz, and E.M. Engler, *Phys. Rev. Lett.* **46**, 1234 (1981).
- <sup>18</sup> K. Mortensen, Y. Tomkiewicz, and K. Bechgaard, *Phys. Rev. B* **25**, 3319 (1982).
- <sup>19</sup> C. Gaonach and G. Creuzet, *Synth. Met.* **16**, 299 (1986).
- <sup>20</sup> G. Creuzet, C. Gaonach, and B. Hamzic, *Synth. Met.* **19**, 245 (1987).
- <sup>21</sup> J.M. Delrieu, M. Roger, Z. Toffano, A. Moradpour, and K. Bechgaard, *J. Phys.* **47**, 839 (1986).
- <sup>22</sup> S. Tomić, J.R. Cooper, W. Kang, D. Jérôme, and K. Maki, *J. Phys. (France) I* **1**, 1603 (1991).
- <sup>23</sup> G. Kriza, G. Quirion, O. Traetteberg, and D. Jérôme, *Europhys. Lett.* **16**, 585 (1991).
- <sup>24</sup> L.P. Le, A. Keren, G.M. Luke, B.J. Sternlieb, W.D. Wu, Y.J. Uemura, J.H. Brewer, T.M. Riseman, R.V. Upasani, L.Y. Chiang, W. Kang, P.M. Chaikin, T. Csiba, and G. Grüner, *Phys. Rev. B* **48**, 7284 (1993).
- <sup>25</sup> J.P. Ulmet, A. Khmou, and L. Bachere, *Synth. Met.* **19**, 271 (1987).
- <sup>26</sup> W. Kang, S.T. Hannahs, and P.M. Chaikin, *Phys. Rev. Lett.* **70**, 3091 (1993).
- <sup>27</sup> W. Kang, S.T. Hannahs, L.Y. Chiang, R. Upasani, and P.M. Chaikin, *Phys. Rev. B* **45**, 13 566 (1992).
- <sup>28</sup> S.E. Brown, B. Alavi, G. Grüner, and K. Bartholomew, *Phys. Rev. B* **46**, 10 483 (1992).
- <sup>29</sup> K. Kornelsen, J.E. Eldridge, and G.S. Bates, *Phys. Rev. B* **35**, 9162 (1987).
- <sup>30</sup> P.M. Chaikin, P. Haen, E.M. Engler, and R.L. Greene, *Phys. Rev. B* **24**, 7155 (1981).
- <sup>31</sup> A. Bjeliš and D. Zanchi, *Phys. Rev. B* **49**, 5968 (1994).
- <sup>32</sup> A. Virosztek and K. Maki, *Phys. Rev. B* **49**, 6074 (1994).
- <sup>33</sup> L.P. Gor'kov and A.G. Lebed', *Phys. Rev. Lett.* **71**, 3874 (1993).
- <sup>34</sup> A. Bjeliš and K. Maki, *Phys. Rev. B* **45**, 12 887 (1992).
- <sup>35</sup> A. Bjeliš and K. Maki, *Phys. Rev. B* **44**, 6799 (1991).
- <sup>36</sup> K. Maki and A. Virosztek, *Phys. Rev. B* **42**, 655 (1990).
- <sup>37</sup> A. Bjeliš and K. Maki, *Phys. Rev. B* **42**, 10 275 (1990).
- <sup>38</sup> G. Montambaux, *Phys. Rev. B* **38**, 4788 (1988).
- <sup>39</sup> K. Yamaji, *Synth. Met.* **13**, 29 (1986).
- <sup>40</sup> K. Yamaji, *J. Phys. Soc. Jpn.* **53**, 2189 (1984).
- <sup>41</sup> K. Yamaji, *J. Phys. Soc. Jpn.* **51**, 2787 (1982).
- <sup>42</sup> W.H. Wong, M.E. Hanson, W.G. Clark, B. Alavi, and G. Grüner, *Phys. Rev. Lett.* **72**, 2640 (1994).
- <sup>43</sup> E. Barthel, G. Quirion, P. Wzietek, D. Jérôme, J.B. Christiansen, M. Jorgensen, and K. Bechgaard, *Phys. Rev. Lett.* **71**, 2825 (1993).
- <sup>44</sup> W.G. Clark, M.E. Hanson, W.H. Wong, and B. Alavi, *J. Phys. (France) IV* **3**, 235 (1993).
- <sup>45</sup> W.H. Wong, M.E. Hanson, B. Alavi, W.G. Clark, and W.A. Hines, *Phys. Rev. Lett.* **70**, 1882 (1993).
- <sup>46</sup> E. Barthel, G. Quirion, P. Wzietek, D. Jérôme, J.B. Christiansen, M. Jorgensen, and K. Bechgaard, *Europhys. Lett.* **21**, 87 (1993).
- <sup>47</sup> T. Takahashi, T. Harada, Y. Kobayashi, K. Suzuki, K. Murata, and G. Saito, *Synth. Met.* **41-43**, 3985 (1991).
- <sup>48</sup> T. Takahashi, Y. Maniwa, H. Kaqamura, and G. Saito, *J. Phys. Soc. Jpn.* **55**, 1364 (1986).
- <sup>49</sup> C. Bourbonnais, P. Stein, D. Jérôme, and A. Moradpour, *Phys. Rev. B* **33**, 7608 (1986).
- <sup>50</sup> J. Coroneus, B. Alavi, and S.E. Brown, *Phys. Rev. Lett.* **70**, 2332 (1993).
- <sup>51</sup> J.C. Lasjaunias, K. Biljakovic, P. Monceau, and K. Bechgaard, *Solid State Commun.* **84**, 297 (1992).
- <sup>52</sup> J.C. Lasjaunias, K. Biljakovic, F. Nad, P. Monceau, and K. Bechgaard, *Phys. Rev. Lett.* **72**, 1283 (1994).
- <sup>53</sup> D. Quinlivan, Y. Kim, G. Grüner, and F. Wudl, *Phys. Rev. Lett.* **65**, 1816 (1990).
- <sup>54</sup> A. Jánossy, M. Hardiman, and G. Grüner, *Solid State Commun.* **46**, 21 (1983).
- <sup>55</sup> K. Maki and G. Grüner, *Phys. Rev. Lett.* **66**, 782 (1991).
- <sup>56</sup> L.I. Buranov and I.F. Shchegolev, *Instrum. Expt. Tech.* **14**, 528 (1971).
- <sup>57</sup> O. Klein, S. Donovan, M. Dressel, and G. Grüner, *Int. J. Infrared Millimeter Waves* **14**, 2423 (1993).
- <sup>58</sup> S. Donovan, O. Klein, M. Dressel, K. Holczer, and G. Grüner, *Int. J. Infrared Millimeter Waves* **14**, 2459 (1993).
- <sup>59</sup> M. Dressel, O. Klein, S. Donovan, and G. Grüner, *Int. J.*

- Infrared Millimeter Waves **14**, 2489 (1993).
- <sup>60</sup> Within the surface impedance approximation, the temperature dependence of  $\frac{\delta\omega}{\omega}$  for a highly conducting sample should follow  $\frac{\alpha}{N}$  quite closely once the thermal expansion has been accounted for. Thus,  $\frac{\delta\omega}{\omega}$  could be considered a measure of the thermal expansion, as suggested in Ref. 59.
- <sup>61</sup> F. Nad (private communication).
- <sup>62</sup> L. Hubert and C. Bourbonnais (unpublished).
- <sup>63</sup> J.P. Ulmet, P. Auban, A. Khmou, and S. Askenazy, J. Phys. (Paris) Lett. **46**, L-535 (1985).
- <sup>64</sup> J.C. Pieri, S. Allen, M. Poirier, and C. Bourbonnais (unpublished).
- <sup>65</sup> L.P. Gor'kov and A.G. Lebed', J. Phys. (Paris) Lett. **45**, L-433 (1984).
- <sup>66</sup> K. Yamaji, J. Phys. Soc. Jpn. **54**, 1034 (1985).
- <sup>67</sup> K.F. Herzfeld and T.A. Litovitz, *Absorption and Dispersion of Ultrasonic Waves* (Academic Press, New York, 1959).
- <sup>68</sup> F. Ya Nad and P. Monceau, Solid State Commun. **87**, 13 (1993).
- <sup>69</sup> G. Kriza, Y. Kim, A. Beleznyay, and G. Mihály, Solid State Commun. **79**, 811 (1991).
- <sup>70</sup> X.D. Shi, A.R. Kortan, J.M. Williams, A.M. Kini, B.M. Savall, and P.M. Chaikin, Phys. Rev. Lett. **68**, 827 (1992).
- <sup>71</sup> W. Schranz, A. Fuith, P. Dolinar, H. Warhanek, M. Haluska, and H. Kuzmany, Phys. Rev. Lett. **71**, 1561 (1993).